Modeling and Numerical Simulation of Afterburning of Thermobaric Explosives In a Closed Chamber

Kyoung su Im, Grant Cook, Jr., and Zeng-Chan Zhang
Livermore Software Technology Corp.

INTRODUCTION

Heterogeneous combustion (i.e., solid and gas or liquid and gas) has a wide range of applications such as solid rocket propulsion, combustion instability control, underwater explosion, and high energy explosion [1-4]. Among several possible combinations, the thermobaric explosive (TBX) composed of trinitrotoluene (TNT) and energetic metal particles (typically aluminum) is a widely used explosive and is of great importance in the safety, mining, and defense industries.

TBX (a thermobaric explosive) is defined as "a partially detonating energetic material with excess fuel (gas, solid or liquid) dispersed and mixed into air with subsequent ignition and reaction achieved in time and in place for added gain of energy, blast and heat." As such, TBX has greatly enhanced thermal and blast effects compared to conventional high explosives [5].

In TBX flow, thermobaric effects are obtained by long-duration overpressure and heating due to the afterburning of detonation products in air. Since the afterburning process is controlled by turbulent mixing and combustion in air after detonation or dispersion by a bursting charge, even the identical explosive composition may yield different thermal and blast performance with different targets. Therefore, the detailed understanding of the afterburning mechanism is required to optimally design warheads for various operational environments. To this end, TBX module has been implemented in in LS-DYNA®

MODEL VALIDATION WITH EXPERIMENT

Experiments in present investigation were carried out using a closed bomb test (CBT) chamber for model validation of the TBX afterburning processes. Figure 1 shows the schematics of the experimental chamber and an initial charge of TBX. The CBT chamber has a dimension of 40 cm in radius (r) and 150cm in longitudinal length (x) so that the total volume of the chamber is 0.754 m^3. Two pressure gauges (Kulite; HEL-375-250A, and HEL-375-500A) having different sensing capacities were installed: one at the front enter of the cylinder (x=750cm, r= 40cm) and the other at the side center of the cylinder base surface (x=150cm, r= 0cm), respectively. The measured pressure data from the sensors were logged using the data acquisition system, DEWE-500, for analysis of the blast performance.

The cylindrical (30 mm in diameter and 33mm in length) Tritonal TBX charge weighs 40g and consists of well mixed TNT (80%) and aluminum particles (20%, with an average diameter of 10μm). The main charge, combined with the blast cap (5g booster explosives of TNT compounds) and the exploding bridge wire (EBW) shown in Fig. 1(b) was initially located at the CBT center (x=75cm, r=0cm) of the CBT chamber for each experiment. Several experiments were conducted to obtain reliable data sets, and three data sets were collected with less than 10% standard relative error (SRE) from the average at each time instant. The pressure histories after explosion are illustrated in Fig. 2 at the side (a) and front center (b) of the CBT chamber.

Figure 2 shows the TBX validations with the pressure data sets for the side and front center position between the simulation results and averaged experimental data. Figure 2(a) and (b) illustrate the pressure history at the side and front center, respectively, and Figure 2(c) and (d) show the corresponding impulse, which is defined as pressure integrated over time. It is clear that the simulation results are in excellent agreement with the experimental data over the time ranges. At earlier time, the peak pressures slightly overshoot the measured data. In general, when the metal particles contribute to the afterburning in TBX, the peak pressure becomes lower but the impulse tends to be higher as the chamber pressure lasts longer than that of normal high explosives.

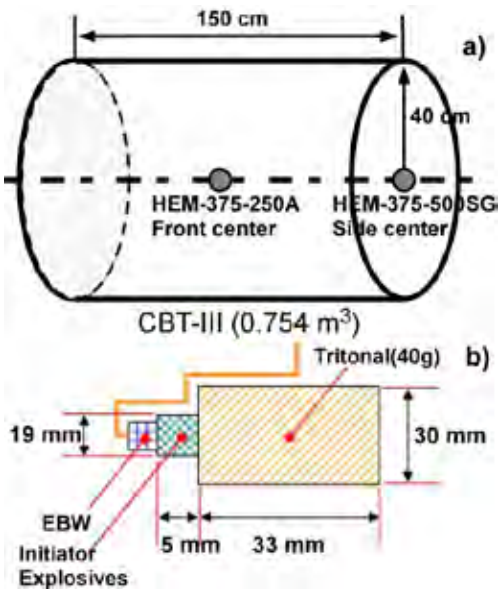

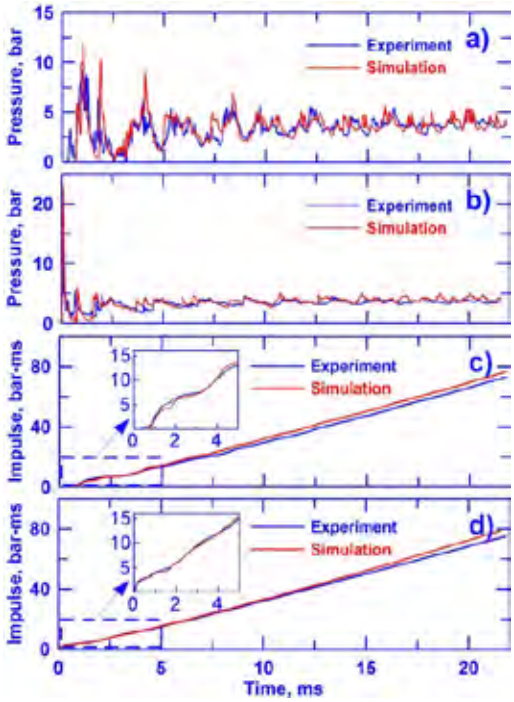

Figure 1 **Figure 2**

Figure 1 Schematics of the experimental closed bomb test chamber and the structure of the initial TBX: a) closed bomb test chamber with volume of 0.754 m^3 with two pressure sensing positions at front and side center, and b) the TBX charge structure consists of 40g of Tritonal and a blasting cap (initiator explosives, and an exploding bridge wire (EBW)).

Figure 2 Comparisons between measured data and simulation at the side and front center positions: a) and b) are the pressure histories, c) and d) are the impulses versus time.

BLAST PERFORMANCE

Prior to TBX simulation, the homogeneous calculation with only TNT explosive was conducted to better understand blast wave propagation and also to validate the developed code. Detailed geometrical setups and initial conditions can be found in Ref. [6]. Although the results are not provided, the over pressure histories in time [6] was validated as a preliminary calculation.

Figure 3 shows consecutive snapshots of the temperature distributions at different time instants showing the blast wave propagation procedures. After symmetric propagation and flame separation from a leading shock in Fig. 3(a) and (b), the shock wave hits the side walls and is reflected (Fig. 3(c)). Then, the flame starts to randomly mix as shown in Fig. 3(d)~3(f). At later times, the flames become more chaotically mixed as seen in Fig. 3(g)~3(i).

When the blast waves arrives at the side center, the pressure immediately peaks to its maximum value, and the reflected wave from the cylinder wall results in the subsequent peaks as the process repeats, conjugates, and dissipates until the pressure converges to an elevated value, but still with considerably noisy patterns after 5ms from the initial explosion.

PARTICLE DYNAMICS

Figure 4 illustrates the effects of particle dynamics on aluminum vaporization by varying the initial conditions such as mono-dispersed and Rosin-Rammler distributions, and different particle mean diameters, 10μm, 20μm, and 40μm. The mono-dispersed distributions show a higher rate of vaporization in all cases. The deviations from the vaporization curves between the distributions are reduced with increasing diameter and eventually, there is little difference in the 40μm cases, in which the size distribution is no longer important in confined explosions. It is also obvious that the vaporization rates decrease almost linearly with increasing diameter. At 10 μm, the particle

vaporization is about 80% of the initial aluminum particle mass. With doubled diameter, it is approximately reduced by factor of two. At 40 μm, it is cut down another half, much less than 20%. From these observations, the maximum contribution of metal combustion to the afterburning performance occurred at small particle diameter. But there might be a critical diameter to optimize the afterburning performance. Therefore, the proper selection of the particle diameter is of paramount importance in the manufacturing process of TBX.

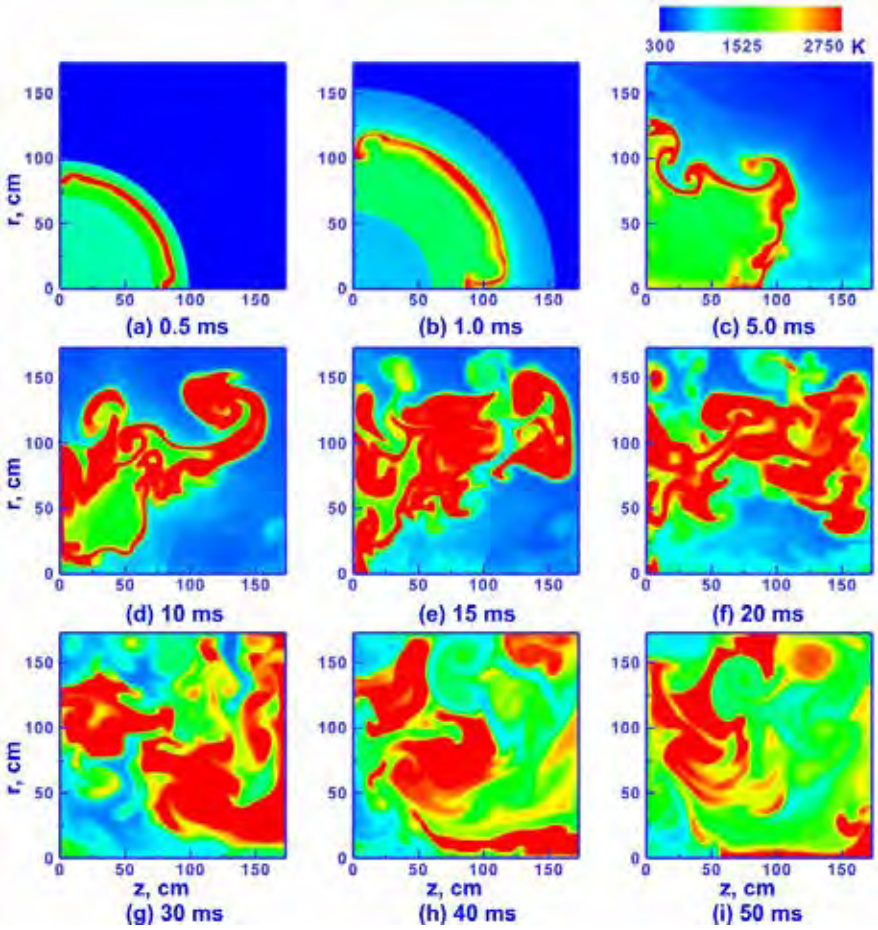

Figure 3 Consecutive snapshots of the temperature distributions at different time for the blast propagation.

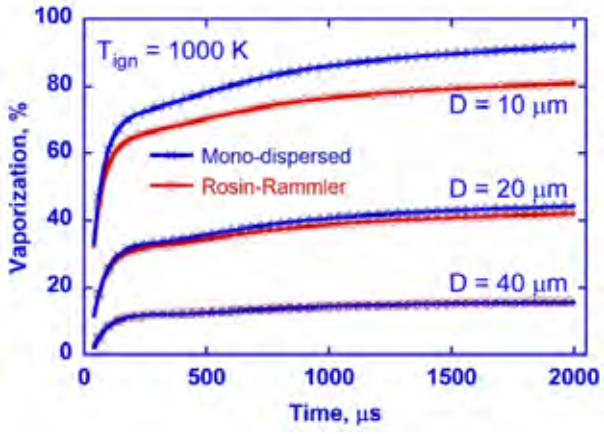

Figure 4 Aluminum vaporization rate according to particle distribution and different particle diameters.

INFORMATION: HOW TO USE

1. Prepare the chemistry input file (*.inp) and thermodynamics data files (thermo.dat) participated combustion species in the calculation.
2. Select the metal partice and set the initial condition using *STOCHASTIC_TBX_PARTICLES.
3. Set initial conditions and chemistry composition for the calculations.
4. Run the code to get the blast performance or TBX flow properties.

CONCLUSION

The present investigation has demonstrated an accurate and concrete model developed for the afterburning process of TBX combustion in conjunction with experimental validation in a confined chamber. The simulation for the afterburning of TBX, validated by the experimental data, clearly revealed the importance of the blast performance and particle dynamics, which should find broader applications in related industries by using the CE/SE and Chemistry solver in LS-DYNA.

REFERENCE

1. K. Kim, W. Wilson, J. Colon, T. Kreitinger, C. Needham, et. al., “Non-ideal explosive performance in a building structure,” WIT Transaction on The Built Environment, 87, pp. 515-524, 2006.
2. J. Massoni, R. Saurel, A. Lefrancois, and G. Baudin, “Modeling spherical explosions with aluminized energetic materials,” Shock Waves, Vol. 16, pp. 75-92, 2006.
3. E. W. Price, K. J. Kraeutle, J. L. Prentice, T. L. Boggs, J. E. Crump, and D. E. Zurn, “Behavior of Aluminum in Solid Propellant Combustion,” NWC TP 6120, 1982.
4. C.-K. Kim, J. G. Moon, J.-S. Hwang, M.-C. Lai, and K.-S. Im , “Afterburning of TNT Explosive Products in Air with Aluminum Particles”, AIAA Paper 2008-1029, 2008
5. A. L. Kuhl, R. E. Ferguson, and A. K. Oppenheim, "Gasdynamics Model of Turbulent Exothermic Fields in Explosions," Progress in Astronautics and Aeronautics Series, 173,AAA, Washington, D.C, pp. 251-261, 1997.
6. D. Schwer, and K. Kailasanath, “Blast Mitigation by Water Mist (1) Simulation of Confined Blast Waves,” Technical Report NRL/MR/6410-02-8636, 2002.